THE JOURNAL OF PHYSICAL CHEMISTRY A

pubs.acs.org/JPCA

Article

Energetics for Proton Reduction in FeFe Hydrogenase

Per E. M. Siegbahn* and Rong-Zhen Liao*

Cite This: *J. Phys. Chem. A* 2020, 124, 10540−10549

Read Online

ACCESS | Metrics & More | Article Recommendations | Supporting Information

ABSTRACT: The energetics for proton reduction in FeFe-hydrogenase has been reinvestigated by theoretical modeling, in light of recent experiments. Two different mechanisms have been considered. In the first one, the bridging hydride position was blocked by the enzyme, which is the mechanism that has been supported by a recent spectroscopic study by Cramer et al. A major difficulty in the present study to agree with experimental energetics was to find the right position for the added proton in the first reduction step. It was eventually found that the best position was as a terminal hydride on the distal iron, which has not been suggested in any of the recent, experimentally based mechanisms. The lowest transition state was surprisingly found to be a bond formation between a proton on a cysteine and the terminal hydride. This type of TS is similar to the one for heterolytic H_2 cleavage in NiFe hydrogenase. The second mechanism investigated here is not supported by the present calculations or the recent experiments by Cramer et al., but was still studied as an interesting comparison. In that mechanism, the formation of the bridging hydride was allowed. The H−H formation barrier is only 3.6 kcal/mol higher than for the first mechanism, but there are severe problems concerning the motion of the protons.

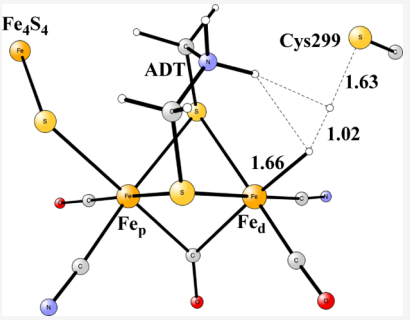

1. INTRODUCTION

FeFe hydrogenases are the leading enzymes in nature for forming hydrogen molecules from protons and electrons. The first X-ray structure appeared in 1998.[1] A model of the structure is shown in Figure 1. The structure is quite unusual with an FeFe dimer connected by a cysteine bridge to an Fe_4S_4 cluster, together termed the H-cluster. The Fe-atom in the dimer closest to the Fe_4S_4 cluster is termed the proximal iron (Fe_p) and the other one the distal iron (Fe_d). As in the case of NiFe hydrogenases, there are CO and CN^- ligands, otherwise very uncommon in nature. Each iron in the Fe-dimer has one terminal CO and one terminal CN^- ligand, and there is also one bridging CO. Furthermore, the two irons are bridged by a five-atom dithiolate ligand not seen before in any enzyme. In the figure, the dithiolate ligand contains a nitrogen atom. However, whether this atom should be assigned as carbon or nitrogen was debated initially, because this could not be deduced from the X-ray structure. There is now consensus that it is a nitrogen atom, and the dithiolate was therefore identified as an aza-dithiolate (ADT).[3,5] The first decade after the X-ray structure, the mechanism for H_2 formation was studied intensively by both experimental and theoretical methods.

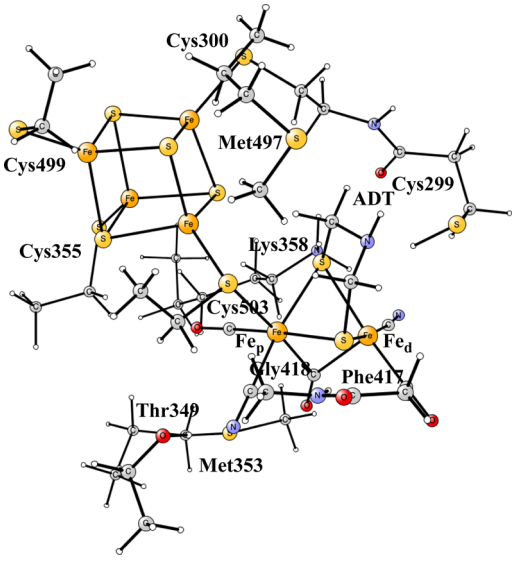

Figure 1. Optimized model used for the active site illustrating which amino acids were included. Starting coordinates were taken from PDB entry 1FEH of *Clostridium pasteurianum* (CpI).[1] The structure is identified as H_{ox}.

The oxidation states appearing in the mechanism were studied by EPR and Mössbauer spectroscopies and by theoretical modeling studies. The early theoretical development was described in a review in 2007.[2] There are three states involved in the mechanism, initially termed H_{ox}^{air}, H_{ox}, and H_{red}. The studies converged to assignment for the di-iron part of the H-

Received: September 24, 2020
Revised: November 24, 2020
Published: December 4, 2020

https://dx.doi.org/10.1021/acs.jpca.0c08705
J. Phys. Chem. A 2020, 124, 10540−10549

cluster with H_{ox}^{air} as Fe_2(II,II), with H_{ox} as Fe_2(I,II) and with H_{red} as Fe_2(I,I). The presence of Fe(I) in the mechanism was unprecedented and was considered as a key for the efficiency of FeFe-hydrogenase in forming hydrogen molecules and was therefore used as a guideline for designing artificial mimics.

For the mechanism, Hall, Hu, and co-workers[3,4] suggested that the formation of H_2 occurs at the distal iron center, while De Gioia et al.[5] suggested that it should occur in the region between the two iron centers in the dimer. Hall and Hu[3,4] suggested that in the first reduction step in the catalytic cycle, there is a binding of a proton to the nitrogen of the dithiolate (ADT) ligand. This structure is in equilibrium with a structure with a terminal hydride on the distal iron and an unprotonated ADT. After addition of a proton in the region of the distal iron and the ADT, in the same reduction step, H_2 is formed. H_2 is released only after a second reduction. De Gioia and coworkers instead suggested that H_2 is formed from a bridging hydride and a proton bound to a sulfur of the dithiolate. Both these leading mechanisms thus suggest that a proton is bound to the dithiolate but differ in the position of the hydride.

In recent years, there has been an increased number of spectroscopic studies of the mechanism for FeFe hydrogenase. Through a combination of nuclear resonance vibrational spectroscopy (NRVS), FTIR spectroscopy, and DFT calculations, Cramer et al.[6] studied a mutated structure, which was interpreted as showing a terminal hydride species on the distal iron, strongly hydrogen bonded to the dithiolate ligand, in good agreement with the mechanism by Hall and Hu described above. Furthermore, using FTIR, nuclear resonance vibrational spectroscopy, and DFT calculations, Lubitz and Cramer et al.[7−10] made observations which also supported that picture but also showed a more direct involvement of the Fe_4S_4 cluster through a redox coupling within the H-cluster. They also showed that Cys299 is the immediate proton donor to the nitrogen of the ADT. Ratzloff et al.[11] were the first to show experimental evidence that there is no loss of the bridging CO between the two irons in the dimer. In the most recent of the spectroscopic studies of FeFe hydrogenase,[12] different intermediate states were observed. Low-temperature IR spectroscopy and nuclear resonance vibrational spectroscopy were used. DFT was used to analyze the experiments. Two of the states in the catalytic cycle were suggested to have two Fe(I) atoms in the Fe-dimer. The main conclusion reached was that the catalytic cycle does not involve bridging hydrides, which was a very surprising conclusion, because DFT calculations in the same study and previously had reported a very high stability of the bridging hydride. The structure was somehow avoided. To block a very stable structure from protonation, suggests a quite unusual mechanism, not seen in any other enzyme, to the best of our knowledge. In all these studies, the H−H bond was suggested to occur between a hydride and a protonated nitrogen of the dithiolate. However, also recently, Haumann et al.[13,14] obtained results by infrared spectroscopy and isotope editing that seemed to contradict the above picture. They showed that the nitrogen of the dithiolate ligand was not protonated in any intermediate, in contrast to both mechanisms described above, where the H−H bond formation occurs with a protonated nitrogen of the dithiolate. The spectroscopic results indicated that in one of the intermediates, the Fe_4S_4 cluster instead becomes protonated, which was suggested to stabilize a reactive, terminal hydride.

A few other studies of interest in the present context have also rather recently been published. In one of them, Mulder et al.[15] used Mössbauer spectroscopy and DFT to define the doubly reduced structure, termed H_{hyd}. They concluded that H_{hyd} is in a Fe_2(II,II) state with a terminal hydride. They suggested a mechanism where the terminal hydride appears for the first time after two reductions. Myers et al.[16] presented a detailed experimental study of the hyperfine interactions in the H_{ox} state that defined the localization of the unpaired spin on Fe_d.

Other mechanistic aspects of FeFe hydrogenases have also been investigated by computational methods. For example, Hall and coworkers[17,18] studied the oxygenated isomers of the di-iron cluster and found that the relative stabilities of the di-iron-bridging oxo complex and the oxygenated sulfur complex are extremely sensitive to the choice of density functional. Reiher and coworkers[19,20] addressed the mechanism of inactivation of this enzyme by O_2 and suggested a protonation mechanism involving water release and degradation of the ligand environment, which could explain the irreversibility of the enzyme inactivation. They have also unraveled the effect of a homogeneous electric field on the reactivity of the active site of this enzyme and suggested that the field at the ligand-binding site is used to tune the reversibility of H_2 oxidation and formation. Greco et al.[21,22] performed QM/MM calculations to understand the electronic structures of the three inorganic clusters and suggested a mixed Fe(II)Fe(I) state in the H-cluster. McCullagh and Voth[23] used a combination of atomistic molecular dynamics, dynamics coarse-graining, and Marcus theory calculations to investigate the electron transfer steps and suggested a proton-coupled electron transfer (PCET) mechanism to the active site. Ginovska-Pangovska et al.[24] performed molecular dynamics simulations to explore the proton transport pathways and suggested a five-residue motif for proton delivery. Sensi et al.[25] investigated the reactivity of the excited state of the H-cluster using combined experimental and TDDFT calculations, focusing on the photochemical binding and release of CO.

In light of the recent studies by Lubitz and Cramer et al.[8−10,12] and those of Haumann et al.,[13,14] a renewed theoretical study of the mechanism was undertaken. Another reason for the present study was to investigate the energetics of the reduction steps where the protons and electrons enter, which had not been studied by theory before. In that context, a comparison to the mechanism of NiFe hydrogenase, recently studied using similar methods as here,[26] was made to investigate similarities and differences of the two enzymatic mechanisms.

2. METHODS

The methods used here are the same as the ones used recently for NiFe hydrogenase and also for many similar enzyme mechanisms.[27] The starting point is the standard B3LYP method,[28] which has 20% exact exchange. By a large amount of experience on enzyme mechanisms, it has been noted that the B3LYP results are almost only sensitive to the exact exchange part. The key for obtaining a handle on the accuracy is therefore to vary this fraction from 20 to 15 to 10%.[29] Thus far, the best agreement with experiments for enzyme mechanisms has been obtained for a fraction of 15−20%. Most notable in this context is the case of water oxidation in PSII, where a fraction of 15% was required to reproduce the experimental PCET redox potentials. The results predicted for the mechanism have been shown to be in excellent agreement with experiments, performed years later.[30]

The geometries are optimized using a LACVP* basis set, which is of moderate DZP size. For the final geometries (single points), a much larger basis set was used with *cc*-pvtz(-f) for the

https://dx.doi.org/10.1021/acs.jpca.0c08705
J. Phys. Chem. A 2020, 124, 10540−10549

nonmetal atoms and with LAV3P* for the metals. Solvation effects were obtained using a Poisson-Boltzmann solver,[31] with a dielectric constant of 4.0. Zero-point effects were obtained from computed Hessians with the LACVP* basis. D3 dispersion[32] was included in the geometry optimization and D2 was used for the final energies.[33] No essential difference was found between the D2 and D3 results. Translational entropy effects of −8.4 kcal/mol were included in the step, where the hydrogen molecule was released; otherwise, they were assumed to be small. The calculations have been performed with the programs Jaguar[31] and Gaussian 09.[34]

The model used for the active site was built from the X-ray structure of *C. pasteurianum* (CpI).[1] The model is shown in Figure 1, to illustrate the atoms included. For the iron dimer part, there are three CO, two CN, and the bridging dithiolate ligands. Outside the dimer, Lys358, Met353, Met497, Thr349, and the backbone parts of Phe417 and Gly418 were included. For the Fe_4S_4 cluster, there are four cysteine ligands, Cys300, Cys355, Cys499, and Cys503. The bridging ligand between the iron dimer and the Fe_4S_4 cluster is Cys503. At a rather late stage, Cys299 was also added to the model, which was found to be quite important. The reason it was not included in the starting model was that it is not a ligand of the H-cluster and is not charged. In cluster modeling, it is necessary to keep some atoms fixed from the X-ray structure.[35] For all amino acids, the α carbon and two hydrogens bound to it were fixed. The details are found in the Supporting Information.

In order to study the reduction processes, it is necessary to have an estimate of the driving force. The redox potential for proton reduction is −0.41 V at pH = 7. Because hydrogenases are optimized to avoid a loss of energy, a small driving force (ΔE) of −3.6 kcal/mol (−0.15 V) was assumed as a reasonable value, corresponding to a redox potential of the electron donor of −0.49 V at pH = 7. A driving force greater than 2.8 kcal/mol leads to a yield of 99%. The overall reaction is as follows

$$2(H^+, e^-) \rightarrow H_2 + \Delta E$$

The cost for obtaining the reducing (H^+, e^-) couple becomes 368.0 kcal/mol for 15% exact exchange, which also includes the translational entropy contribution of 8.4 kcal/mol. To obtain the same driving force, a value of 366.7 kcal/mol was used for 10% and 369.5 kcal/mol for 20%. The differences are entirely because of the different energies for the H_2 molecule. For the oxidation of H_2, a driving force of −3.6 kcal/mol corresponds to a redox potential of −0.34 V for the electron acceptor at pH = 7. Under the conditions used in the spectroscopic studies, the cost of the reducing (H^+, e^-) couple becomes 367.1 kcal/mol for 15%. To obtain a reference value for individual electron and proton transfers to the H-cluster requires one single parameter obtained from experimental information, just as for PSII.[30] In the present case, this is not needed because the reductions are proton-coupled.[13] Therefore, only the results for the addition (or subtraction) of (H^+, e^-) couples are reported below.

3. RESULTS

The mechanism for FeFe-hydrogenase has been studied by DFT using the B3LYP functional with 20, 15, and 10% exact exchange. Most of the results discussed below have been obtained with 15%. The discussion mostly concerns the reduction of protons to H_2, but the reverse reaction of oxidation of H_2 to protons are also discussed. The reduction reaction is of higher interest in the context of using light and water for obtaining H_2 as fuel.

The starting point of the study is the X-ray structure, with the molecular model shown in Figure 1. This structure has been assigned to H_{ox}. The optimized structure is shown also in Figure 2. An interesting feature is that the distal iron (Fe_d) of the Fe-

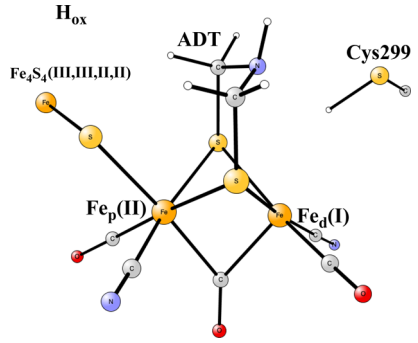

Figure 2. Optimized structure of H_{ox} with a charge of −3 for the H-cluster. The oxidation state of the iron dimer is Fe_2(II,I), and the total spin is a doublet. Atoms not directly involved are not shown.

dimer has an open coordination site. H_{ox} has a −3 charge of the H-cluster, an oxidation state of the dimer Fe_2(II,I), and a doublet total spin-state. The presence of Fe(I) (on Fe_d) has not been seen in any other enzyme, to the best of our knowledge, but the situation here is different with the unusual CN^- and CO ligands and a large negative charge of −3 for the H-cluster. The oxidation state of the Fe_4S_4 cluster is Fe_4(III,III,II,II) with antiferromagnetic coupling between the irons. It has 9α electrons delocalized on one Fe_2(II,III) pair and 9β electrons delocalized on the other pair, forming a broken-symmetry open-shell singlet. The reason water does not bind to Fe_d is that the oxidation state is Fe(I). If there would have been an oxidation state of Fe(II) for Fe_d, water would bind strongly, because Fe(II) prefers an octahedral coordination, see below, which is not the case for Fe(I). To send an electron from Fe_d to the Fe_4S_4 cluster, to change Fe_d to Fe(II), is too costly without a simultaneous protonation of the Fe_4S_4 cluster. As a final test for the structure of H_{ox}, a hydrogen bond from Cys299 to ADT was tried, but the energy was slightly worse than for the structure in Figure 2.

3.1. Mechanism Involving a Blocked Bridging Hydride Position. An important point in the experiments by Cramer and Lubitz et al.[7−10,12] is that a bridging CO is retained during catalysis. This conclusion was based mainly on the finding by IR and NRVS that the characteristic frequency for a bridging CO is present in all structures studied. All DFT calculations done so far, including the ones in the recent study,[12] agree that the energy is much lower for the bridging hydride structure, than for the structures observed in the experiments, and it was therefore concluded that the bridging hydride position is blocked. In the first mechanism studied here, the assumption that the formation of the bridging hydride is blocked is adapted. The conclusion that a structure with a deep minimum is avoided in a mechanism is very unusual and, to the best of our knowledge, has not been seen in any other enzyme.

In the present study, the state obtained after the first reduction by an (H^+, e^-) addition is termed $H_{red}H^+$ and the state obtained after the second reduction is termed H_{hyd}, following the nomenclature used by Haumann and Stripp[13] This does not mean that the structures of these two states are suggested to be the same as the ones suggested by Haumann et al.

To find the optimal structure after the addition of the first (H^+, e^-) couple, to reach $H_{red}H^+$, turned out to be very difficult.

https://dx.doi.org/10.1021/acs.jpca.0c08705
J. Phys. Chem. A 2020, 124, 10540−10549

$H_{red}H^+$ has been observed in both of the recent experimental studies, indicating an exergonic or weakly endergonic transition from H_{ox}. The suggestion by Haumann et al. was that the proton should be added to the Fe_4S_4 cluster, the optimal position being at Cys499. In contrast, Cramer and Lubitz et al. suggested that ADT should be the preferred position. Both these positions, and many more, were tried here without leading to acceptable energies compared to experimental observations. It was always found that the cost for adding the (H^+, e^-) couple to H_{ox} was much too high. To place the proton on Cys499 was found to be as endergonic as +12.9 kcal/mol. Other sulfide positions were found to give quite similar energies. Even considering possible problems with DFT, this suggestion must be ruled out. Placing the proton on ADT was found to be the same with a large endergonicity of +12.9 kcal/mol, and can therefore be ruled out, as well. These results led to explorations of very different mechanisms, but without success.

The final solution to this problem was found when also other positions for the proton were studied, initially considered to be very unlikely. To find a position with a lower energy by more than 10 kcal/mol is necessary to get agreement with the experiments showing that H_{red} H^+ should be observed. One of the more unlikely positions for the proton in H_{red} H^+ was to place the proton as a terminal hydride in the open site of Fe_d. In the formation of this terminal hydride, one electron is taken from the dimer and the other one from the reduction in this step. The oxidation state of the dimer is Fe_2(II,II), while it remains at Fe_4(III,III,II,II) for the Fe_4S_4 cluster. A terminal hydride so early in the mechanism was not suggested in any of the recent, experimentally based mechanisms, but only later in the process after the next reduction. There are early theoretical studies that suggested a terminal hydride at an early stage, but those studies did not consider the energetics for the reduction steps. Contrary to our expectations, the terminal hydride position actually gave a remarkable energy lowering of −13.9 kcal/mol compared to the previous suggestions of Cys499 by Haumann et al. It is also lower in energy by −13.9 kcal/mol than the ADT position, suggested by Cramer and Lubitz et al. The structure is shown in Figure 3. As seen in the figure, there is a strong alternative

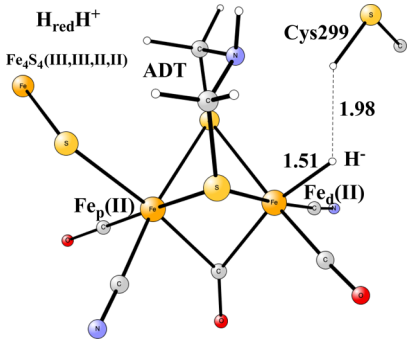

Figure 3. Structure of H_{red} H^+ with a charge of −3 for the H-cluster. The oxidation state of the iron dimer is Fe_2(II,II). The total spin is a singlet. Atoms not directly involved are not shown.

hydrogen bond[36] between the negative hydride and the positive proton on Cys299, stabilizing the hydride. The bond was not present in our initial investigations, because Cys299 was not included in the model. However, even without the hydrogen bond, the position of the proton as a terminal hydride on Fe_d was found to be the optimal position. From the results, the effect of the alternative hydrogen bond on the transition energy from H_{ox} to $H_{red}H^+$ can be estimated to be −4.5 kcal/mol, a substantial and necessary effect on the mechanism. It should be noted that, even after the finding of the quite stable structure for $H_{red}H^+$, a bridging hydride is much lower in energy than the terminal hydride by −17.8 kcal/mol. Therefore, the bridging hydride structure still has to be blocked by the enzyme.

In the next addition of a (H^+, e^-) couple, the H_{hyd} state is reached from H_{red} H^+. H_{hyd} has also been observed in the two experimental studies as mentioned above. The oxidation state of the dimer remains at Fe_2(II,II). The electron is added to the Fe_4S_4 cluster, leading to an oxidation state of Fe_4(III,II,II,II). This is the lowest oxidation state found in the catalytic cycle for the Fe_4S_4 cluster. The added proton here is found to be preferably placed at a ligand (Cys499) bound to the Fe_4S_4 cluster, which is expected because the cluster has been reduced. This is in agreement with the suggestion in the study by Haumann and Stripp.[13] The optimized structure for H_{hyd} is shown in Figure 4. The transition from H_{red} H^+ to H_{hyd} was

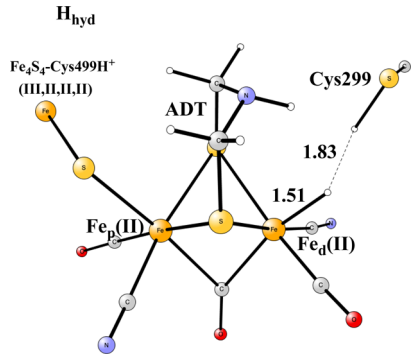

Figure 4. Structure of H_{hyd} with a charge of −3 for the H-cluster. The oxidation state of the iron dimer is Fe_2(II,II). The total spin is a doublet. Atoms not directly involved are not shown.

found to be endergonic by +4.2 kcal/mol. Because the structure has been observed, this result might indicate a minor error of DFT. However, it is also possible that a slightly endergonic state could actually be observed, depending on the experimental detection level.

The next step in the mechanism is to proceed to the TS for H−H bond formation. First, the proton has to move from Cys499 to ADT, which is endergonic by +5.4 kcal/mol. Because the proton transfer leads to an electron transfer from the Fe_4S_4 cluster to the dimer, a future modeling of the proton transfer pathway has to involve the direct coupling to the electron transfer, which is quite difficult to model. To model that has not been done in any earlier studies of the mechanism, and would also require a larger model, including the addition of several water molecules, and was not done in the present study either. The spin on the resulting Fe_2(I,II) dimer is delocalized but is mainly on Fe_p, with a spin of 0.52. The structure is shown in Figure 5 and is here termed H'_{hyd}. After the oxidation of the Fe_4S_4 cluster, the oxidation state becomes Fe_4(III,III,II,II). The most interesting feature of the structure is that there are strong interactions involving three hydrogens, the hydride, the ADT proton, and the proton on Cys299. The distances between the hydrogens are remarkably short, with 1.66 and 1.56 Å.

As seen on the structure of H'_{hyd}, there may be two possibilities to reach a TS for H−H bond formation. The first one is shown in Figure 6 and is the one suggested in many earlier studies of the mechanism. At the TS, the distance between the hydrogens is

https://dx.doi.org/10.1021/acs.jpca.0c08705
J. Phys. Chem. A 2020, 124, 10540−10549

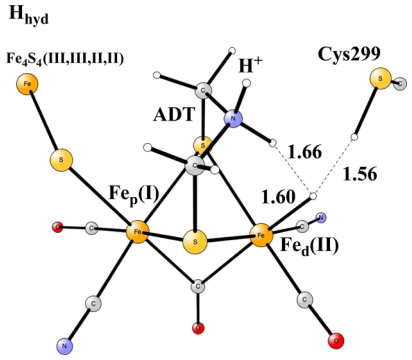

Figure 5. Structure of H'_{hyd} with a charge of −3 for the H-cluster. The oxidation state of the iron dimer is Fe_2(I,II). The total spin is a doublet. Atoms not directly involved are not shown.

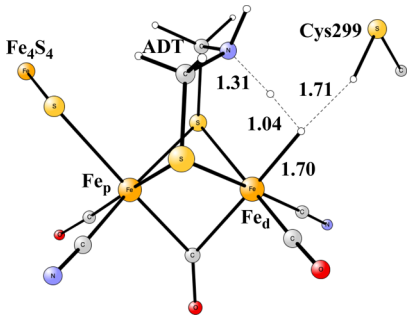

Figure 6. Transition state for the H−H bond formation with a charge of −3 for the H-cluster. The oxidation state of the iron dimer is Fe_2(II,I). The total spin is a doublet, and the charge of the H-cluster is −3. Atoms not directly involved are not shown.

1.04 Å, the distance between ADT and the proton has increased from 1.05 to 1.31 Å, and the distance between Fe_d and the hydride has increased from 1.60 to 1.70 Å. The distance from the Cys299 proton and the hydride has increased from 1.56 to 1.71 Å, indicating that it is involved in the mechanism. The local barrier from H'_{hyd} is only 3.1 kcal/mol.

From the structure of H'_{hyd} in Figure 5, there is also another possible TS which is more unexpected. The H−H bond could be formed between the Cys299 proton and the terminal hydride. It turns out that this is actually a slightly preferred TS with a local barrier from H'_{hyd} of 1.8 kcal/mol, 1.3 kcal/mol lower than the one for the mechanism described above. The energy difference is quite small and within the uncertainty of the present calculations. The TS structure is shown in Figure 7. The barrier from H_{hyd} is 7.2 (=5.4 + 1.8) kcal/mol. The distance between the hydrogens is 1.02 Å. The Cys299-H distance has increased to 1.63 Å and the hydride-Fe_d distance to 1.66 Å. The hydrogen on ADT forms rather short unconventional hydrogen bonds to the two hydrogens involved in the bond formation, with distances of 1.89 and 2.16 Å, indicating a charge stabilization of the TS. However, the most important aspect of the added proton on ADT is that it forces a Fe(I) oxidation state on the iron dimer. It should therefore be emphasized that both these mechanisms are in agreement with experiments showing that ADT is an important part of the mechanism.[37] Experiments cannot observe a TS directly and can therefore not be used to indicate the preferred TS. In H'_{hyd} and the two TS, the electron is equally localized on both irons in the dimer, with a sum of the spins of 0.7. It can be added that after the TS, the proton goes immediately over to Cys299 to form H_{ox}.

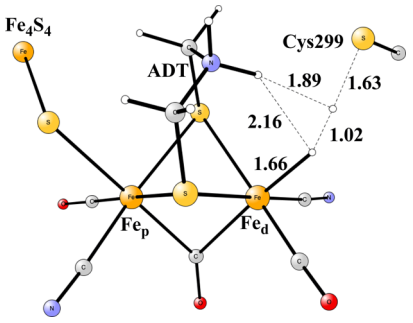

Figure 7. Alternative transition state for the H−H bond formation with a charge of −3 for the H-cluster. The oxidation state of the iron dimer is Fe_2(II,I). The total spin is a doublet, and the charge of the H-cluster is −3. Atoms not directly involved are not shown.

There is an interesting similarity between the lowest TS in Figure 7 and a TS in NiFe hydrogenase. In both cases, the H−H bond is formed between a metal bound hydride and a protonated cysteine via a heterolytic mechanism.

The energies discussed above, using 15% exact exchange, are shown in Figure 8. The most important energy for the

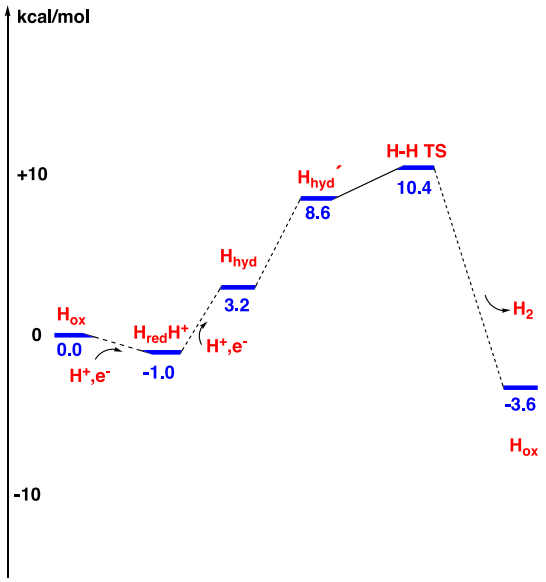

Figure 8. Energy diagram for the mechanism for reduction of protons in the case of a blocked bridging hydride, using 15% exact exchange and a charge of the H-cluster of −3.

mechanism is the total barrier of +11.4 (=10.4 + 1.0) kcal/mol from the resting H_{red} H^+ state. It is also important for the mechanism that the energies for the two reduction steps are not lower than the final point at −3.6 kcal/mol, which would otherwise increase the barriers for the following cycles. In the final step of H_2 release, the increase of the entropy for the free H_2 of −8.4 kcal/mol contributes significantly. No bound molecular H_2 state was found when entropy was added. It should also be noted that the steps between the states marked in the figure must be very efficient, not to increase the overall barrier over +11.4 kcal/mol, in particular for the step between H_{hyd} and H'_{hyd}, where a proton moves from Cys499 to ADT. A proton transfer TS higher by more than +1.8 kcal/mol compared to H'_{hyd} would increase the overall barrier.

https://dx.doi.org/10.1021/acs.jpca.0c08705
J. Phys. Chem. A 2020, 124, 10540−10549

The usual test of the accuracy by using different fractions of exact exchange has been made also in the present case. The results using 15% in Figure 8 are in sequence: 0.0, −1.0, +3.2, +8.6, +10.4, and −3.6 kcal/mol. For 20% exchange (normal B3LYP), the values are 0.0, +3.1, +5.4, +11.9, +14.0, and −3.6 kcal/mol with an overall barrier of +14.0 compared to +11.4 kcal/mol for 15% exact exchange. The barriers for the coming cycles will be the same, because no level is lower than the final one of −3.6 kcal/mol. For 10%, the values are 0.0, −5.1, +1.2, +4.9, +6.3, and −3.6 kcal/mol with an overall barrier of +11.4 (=6.3 + 5.1) kcal/mol. However, because the energy for $H_{red}H^+$ of −5.1 is lower than the final point of −3.6 kcal/mol, the barriers for the coming cycles will be increased by this difference of +1.5 to +12.9 kcal/mol. The overall barriers for 10, 15, and 20% are +12.9, +11.4, and +14.0 kcal/mol. The values are thus quite similar, and the differences do not affect the mechanism or the assignments.

Finally, two other commonly used functionals were used to calculate the single-point energies for $H_{red}H^+$ and H_{hyd}. The energy to obtain a (H^+e^-)-couple was first adjusted to give the same driving force for these functionals as the one used above for B3LYP. For the PW6B95-D3 functional,[38] the energy was found to be +2.3 kcal/mol for $H_{red}H^+$ and for H_{hyd} +12.3 kcal/mol, while for the PBE0-D3 functional,[39] the corresponding values were +1.6 and +8.3 kcal/mol. Because these states have been observed experimentally, they should have energies not higher than +3 kcal/mol, and the accuracies for these functionals are therefore not sufficient for the mechanism studied here. However, both functionals agree with the ones above (B3LYP with different fractions) that $H_{red}H^+$ should have a hydride on Fe_d and not a proton on a cysteine of the Fe_4S_4 cluster as has been suggested by spectroscopic analysis based on calculated frequencies.[13] The latter frequency approach has not been as well tested as the one used here with calculated energies.[40]

The above mechanism relies on the possibility of blocking the formation of the bridging hydride, because there will be a competition between bridging hydride formation and the overall rate of catalysis. The experiments clearly show that the rate of catalysis is indeed faster than that of forming the bridging hydride. To actually calculate the rate of bridging hydride formation is quite difficult, because there are many possibilities. There has actually been an attempt to calculate the barrier for forming the bridging hydride position. Reiher et al.[38] investigated two possible protonation pathways. The first pathway studied was the one from a terminal to a bridging position. It was found to have a very high barrier of +29 kcal/mol, but only an internal transfer was investigated, involving a large structural rearrangement of the ligands. The second protonation pathway investigated, leading to a bridging hydride, was deprotonation of a nearby lysine. Lysine has a very high pK_a and furthermore requires a release from the salt bridge to a cyanide. The pathway was therefore found to be endergonic and to have a very high barrier of +39 kcal/mol.

In a study of the efficiency of blocking the bridging hydride formation, the most critical point is the addition of the first (H^+, e^-) couple. The question here is how much lower the barrier is for hydride formation at a terminal position compared to one at a bridging position, where the latter position is energetically strongly preferred. The number of possible pathways is numerous, for example, involving outside water molecules which is a common way to move protons in enzymes. Such a very difficult study could possibly be a future project.

The calculated energies for reduction can also be used to study the reverse reaction of oxidation. The energy diagram is shown in Figure 9 for 15% exact exchange. The barrier is 14.0

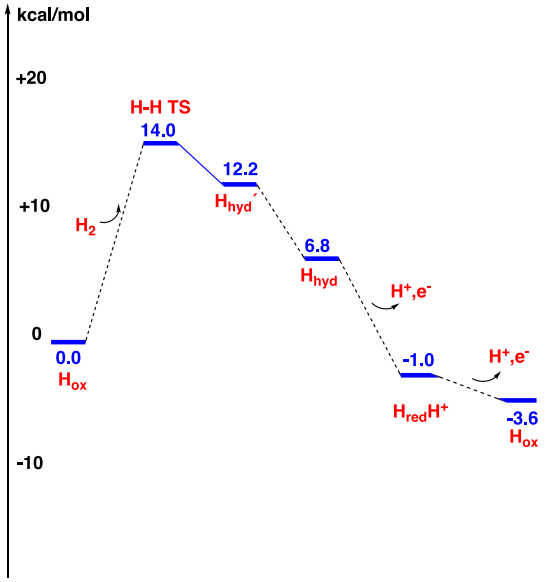

Figure 9. Energy diagram for oxidation of H_2 using 15% exact exchange and a charge of the H-cluster of −3. The bridging hydride position is blocked.

kcal/mol compared to 11.4 kcal/mol for reduction, a substantial difference showing that FeFe hydrogenase is mainly used for reduction. The oxidation barrier is very similar to the one recently computed for NiFe hydrogenase using a heterolytic cleavage mechanism.

3.2. Mechanism Involving a Bridging Hydride. Blocking a position that is very low in energy is extremely unusual in enzyme mechanisms; in fact, it has never been observed in any mechanism studied theoretically before. It is therefore of high interest to investigate what would happen if that position was not blocked. If the charge of the H-cluster is chosen as −3, like in the case of the mechanism discussed above, the bridging hydride would bind very strongly and the process would end up at that point. However, a charge of −3 is far from obvious. In fact, such a large negative charge for a cluster is very unusual, in particular, when there is only one positive residue in the immediate surroundings of the cluster. The study of the case where the bridging hydride is not blocked was therefore done with a charge of the H-cluster of −2. This would lead to a starting structure, here termed H_A, with an oxidation state of Fe_2(II,II) for the iron dimer. The oxidation state of the Fe_4S_4 cluster is Fe_4(III,III,II,II), the same as for H_{ox} described above. The optimized structure is shown in Figure 10. Water binds quite strongly to the distal iron with a Fe−O bond distance of only 2.01 Å. The reason for the strong binding is that Fe(II), unlike Fe(I), prefers an octahedral coordination; see above.

If the H-cluster is reduced by adding a (H^+, e^-) couple, the added hydrogen would bind as a bridging hydride trans to the dithiolate ADT, assuming that the position is not blocked. The optimized structure, termed H_B, is shown in Figure 11. The reduction is exergonic by −5.0 kcal/mol. The spins are still zero for the dimer, indicating that the oxidation state is Fe_2(II,II). The bridging hydride structure is quite strongly preferred, by −13 kcal/mol, compared to protonation of a cysteine on Fe_4S_4. There would be a structural change associated with binding the

https://dx.doi.org/10.1021/acs.jpca.0c08705
J. Phys. Chem. A 2020, 124, 10540−10549

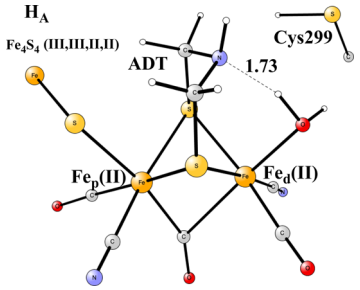

Figure 10. Structure of H_A with a water molecule bound to the distal iron. The oxidation state of the iron dimer is Fe_2(II,II). The total spin is a singlet, and the charge of the H-cluster is −2. Atoms not directly involved are not shown.

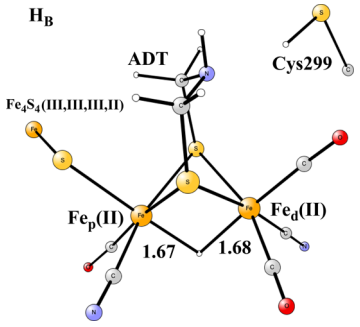

Figure 11. H_B structure obtained after addition of one proton and one electron to H_A. The oxidation state of the iron dimer is Fe_2(II,II). The total spin is a doublet, and the charge of the H-cluster is −2. Atoms not directly involved are not shown.

hydride. The water leaves, and the bridging CO moves to a distal position on Fe_d. Moving the CO forces the other CO on the distal iron to take the position previously held by the water. The oxidation state of the Fe_4S_4 cluster becomes Fe_4(III,III,III,II) still with antiferromagnetic coupling between the irons. The spins are totally delocalized [10α electrons on one pair of Fe_2(III,III) and 9β electrons on the other pair of Fe_2(III,II)]. One of the two electrons on the hydride would come from the Fe_4S_4 cluster.

If there is yet another reduction of the H-cluster by adding a (H^+, e^-) couple, the proton would end up on Cys499 bound to the Fe_4S_4 cluster. Several other protonation sites of the Fe_4S_4 cluster were also tried, including the bridging sulfides, but Cys499 was the best one. Also this reduction is exergonic, now by −2.3 kcal/mol. The optimized structure, termed H_C, is shown in Figure 12. The reduction would occur on the Fe_4S_4 cluster, which should now have the oxidation state Fe_4(III,III,II,II). The oxidation state of the dimer would still be Fe_2(II,II). Thus far, there is no indication of any Fe(I) oxidation state of the dimer.

The next step in the mechanism would be to move the proton from Cys499 to the nitrogen of the bridging dithiolate and to move the bridging hydride to a terminal position on Fe_d; see Figure 13. This change of structure would be needed to prepare the dimer for H−H bond formation. To move the hydride to the terminal position would not be a trivial step. However, the transfer does not necessarily occur by a rotation of the structure. A more likely pathway would be to move the bridging hydride back to the Fe_4S_4 cluster, and then, from there, to the terminal position. However, the pathway is still expected to lead to a high barrier. The thermodynamics of the transfer step is only uphill by +5.8 kcal/mol. There is no change of the oxidation state of

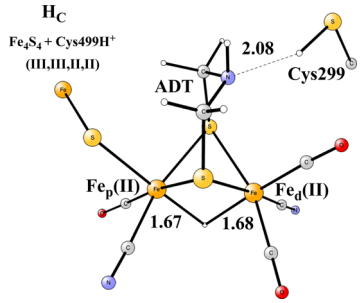

Figure 12. Structure of H_C obtained after addition of one proton and one electron to H_B. The added proton is bound to Cys499, which is a ligand of the Fe_4S_4 cluster. The oxidation state of the iron dimer is Fe_2(II,II). The total spin is a singlet, and the charge of the H-cluster is −2. Atoms not directly involved are not shown.

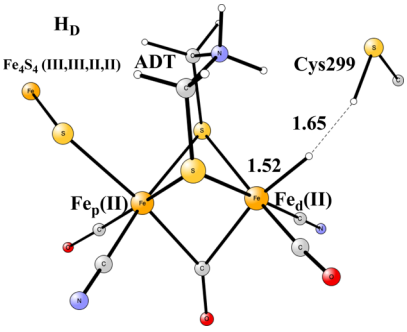

Figure 13. Structure of H_D with a protonated ADT and a terminal hydride. The oxidation state of the iron dimer is Fe(II,II). The total spin is a singlet, and the charge of the H-cluster is −2. Atoms not directly involved are not shown.

the dimer by this change of hydride position, and the oxidation state would therefore still be Fe_2(II,II). The distance between the proton on ADT and the terminal hydride is 2.14 Å. There is a strong alternative hydrogen bond for the structure in Figure 13, just like in the mechanism discussed above for the blocked bridging hydride. The bond distance from the hydride to the Cys299 proton is only 1.65 Å.

The transition state for H−H bond formation is shown in Figure 14. The distance between the hydride and the proton has now decreased to 0.91 Å. The barrier from H_C is 15.0 kcal/mol. After the TS, there is a very flat region at a similar energy as the TS with a binding of H_2 to Fe_d. Unlike the case discussed above for a blocked bridging hydride position, H_2 would not be easily released. The reason for this difference is that the oxidation state

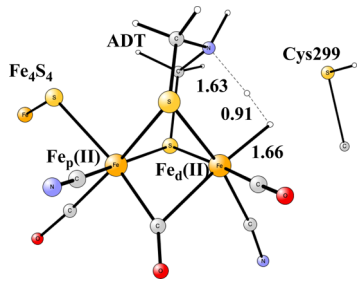

Figure 14. Transition state for the H−H bond formation. The oxidation state of the iron dimer is Fe_2(II,II). The total spin is a singlet, and the charge of the H-cluster is −2. Atoms not directly involved are not shown.

https://dx.doi.org/10.1021/acs.jpca.0c08705
J. Phys. Chem. A 2020, 124, 10540−10549

of Fe_d in the dimer in Figure 14 is Fe(II), which does not like to be five-coordinated in contrast to the case of Fe(I). To complete the catalytic cycle by releasing H_2 would therefore be more complicated, requiring another reduction by adding (H^+, e^-), forming H_B of the next cycle. The proton would be added as a bridging hydride, leading to a six-coordinated Fe_d even after H_2 release. The step from H_D is exergonic by −7.1 kcal/mol. A water molecule might be involved in the reduction step, first forming H_A before the reduction. A more likely scenario would be that the water bound structure should not be involved in the catalytic cycling. The final driving force for the catalytic cycle is −3.6 kcal/mol, as above.

The alternative to form the H−H bond between the hydride and the Cys299 proton was also tried. Shortening the H−H distance leads to a very flat potential surface all the way to a very short H−H distance of 1.0 Å, which at first appears to generate an even lower barrier than for the case where the proton was taken from the nitrogen of the dithiolate. However, this reaction path never releases H_2 without making major structural changes. The reason is that the product with an unprotonated Cys299 is very unfavorable energetically in this case and would therefore bind to the empty site on Fe_d, which is Fe(II). It should be noted that the same problem does not occur for the case with the blocked hydride, because Fe_d is Fe(I), which does not require six-coordination.

The computed energy diagram for proton reduction with a charge of the H-cluster of −2, where the hydride position is not blocked, is shown in Figure 15 for the case of using 15% exact

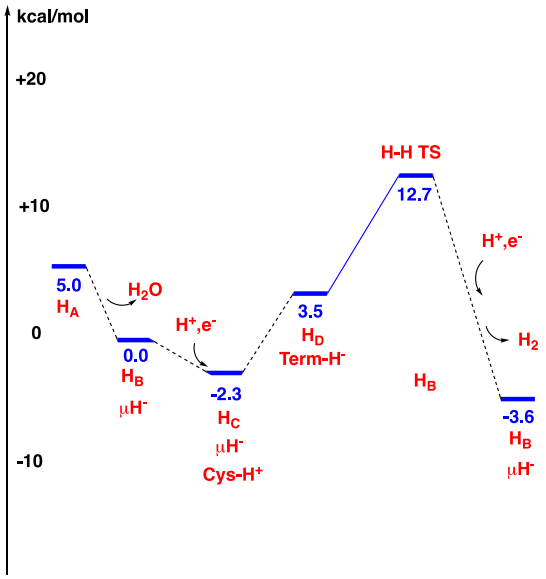

Figure 15. Energy diagram for the reduction of protons using 15% exact exchange, where the bridging hydride position (termed Br−H^-) is not blocked and the H-cluster has a charge of −2.

exchange. The rate-limiting barrier is +15.0 (=12.7 + 2.3) kcal/mol. The mechanism in Figure 15, with the rather low barrier, would be hard to rule out, without the experimental demonstration that a bridging CO is always present in the mechanism.[12] It is quite remarkable that the energy levels of the intermediates are so close in energy, without any deep minima on the pathway, even though the mechanism is not used by the enzyme. It is also interesting that the barrier is so low, with a mechanism that keeps the oxidation state of the dimer as Fe_2(II,II) along the entire cycle. The bridging hydride appears already in the H_B state and is present also in H_C.

4. DISCUSSION AND CONCLUSIONS

The mechanism of proton reduction in FeFe-hydrogenase has been investigated by theoretical modeling techniques. Two different mechanisms have been studied. For the first case, where the position for a bridging hydride is blocked and with a charge of the H-cluster of −3, a mechanism is found that agrees with available experimental thermodynamics and kinetics. The most difficult step to reach agreement for turned out to be the first reduction, in which $H_{red}H^+$ was formed. There have been two recent different experimental suggestions for the protonation site in this reduction. In the first one,[8−10,12] a protonation of the nitrogen of the bridging dithiolate was considered most likely. In the second, vibrational spectroscopy experiments instead led to the conclusion that there should be a protonation of a cysteine on the Fe_4S_4 cluster.[13,14] Surprisingly, after investigating many different possibilities, the calculations instead gave a large preference for forming a terminal hydride on the distal iron (Fe_d) of the Fe_2 dimer, in the first reduction. The preference is so large, 13.9 kcal/mol, that the result for the preferred protonation site must be considered as quite certain. In the second reduction, forming H_{hyd}, the preferred protonation site is on one of the cysteines on the Fe_4S_4 cluster, in agreement with the experimental suggestion by Haumann et al.[13,14]

The preferred TS for H_2 formation gave another unexpected result. In agreement with most suggestions, prior to forming the TS, the proton moves to the nitrogen of the bridging dithiolate, forming $H_{hyd'}$. $H_{hyd'}$ was found to have a surprising structural feature with two very short unconventional hydrogen bonds to the terminal hydride, one from the added proton on the nitrogen of the dithiolate and another one from the proton on Cys299. The proton on the nitrogen of the dithiolate appears not to be used for forming H_2, and the slightly preferred possibility instead forms the H−H bond between a proton on Cys299 and the terminal hydride. This mechanism has strong similarities to the one for heterolytic cleavage in NiFe hydrogenase,[26] where the H−H bond is cleaved between a (bridging) hydride and a proton on a cysteine. The presently calculated barrier is very low with only 11.4 kcal/mol.

In the second mechanism studied, the bridging position is not blocked for hydride formation. The mechanism is not supported by experiments, but was studied anyway for comparison. The preferred charge of the H-cluster in this case is −2. The rate-limiting barrier found is 15.2 kcal/mol compared to 11.4 kcal/mol for the first mechanism. The difference of only +3.8 kcal/mol may be considered surprising. Still, this difference of +3.8 kcal/mol is the reason the enzyme has blocked the pathway to the bridging position. If the energy difference would have been negative, it would have been very easy for the enzyme to organize a pathway to the bridging position by placing suitable amino acids along the pathway.

To understand the mechanism, it is very important to consider also the reduction steps, which have here been studied energetically for the first time. In order to optimize the overall rate, the reduction steps have to be close to isogonic, which could be one reason the unusual structure with cyanide and carbonyl ligands was chosen by nature.

Comparisons have been made here to the mechanism of NiFe hydrogenase, recently studied by similar techniques; see Figure 16.[26] The rate-limiting barriers for oxidation in NiFe hydrogenase, using a heterolytic cleavage mechanism, and for

https://dx.doi.org/10.1021/acs.jpca.0c08705
J. Phys. Chem. A 2020, 124, 10540−10549

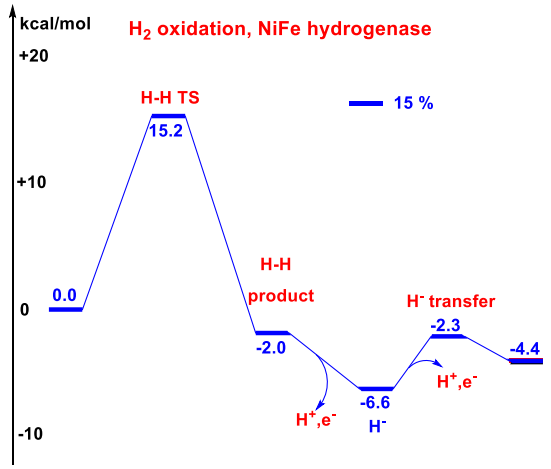

Figure 16. Energy diagram for H_2 oxidation in NiFe-hydrogenase.[26] The mechanism shown is the one for heterolytic cleavage.

oxidation in FeFe hydrogenase with a charge of −3, are very similar. Another similarity is that the oxidations are almost isogonic, which is optimal for this type of process. A difference is that in NiFe hydrogenase, the H−H cleavage directly leads to an exergonic product, while in FeFe hydrogenase, another oxidation is needed to reach an exergonic product.

Another purpose of the present study has been to continue to investigate the accuracy of DFT for redox enzyme mechanisms. Good agreement with experiments is obtained for the energetics. To further test the accuracy, the calculations of the reaction scheme have been calculated for different fractions of exact exchange in the B3LYP functional, for the case of a −3 charge of the H-cluster. The resulting rate-limiting barriers are quite insensitive to this fraction, which indicates a high accuracy of the results. As for other reactions studied, it is found that a fraction of 15% generally gives results in very good agreement with experiments.

■ ASSOCIATED CONTENT

Supporting Information

The Supporting Information is available free of charge at https://pubs.acs.org/doi/10.1021/acs.jpca.0c08705.

Coordinates for all structures (PDF)

■ AUTHOR INFORMATION

Corresponding Authors

Per E. M. Siegbahn − *Department of Organic Chemistry, Arrhenius Laboratory, Stockholm University, SE-106 91 Stockholm, Sweden;* orcid.org/0000-0001-7787-1881; Email: per.siegbahn@su.se

Rong-Zhen Liao − *Key Laboratory for Material Chemistry for Energy Conversion and Storage, Ministry of Education, Hubei Key Laboratory of Bioinorganic Chemistry and Materia Media, Hubei Key Laboratory of Materials Chemistry and Service Failure, School of Chemistry and Chemical Engineering, Huazhong University of Science and Technology, 430074 Wuhan, China;* orcid.org/0000-0002-8989-6928; Email: rongzhen@hust.edu.cn

Complete contact information is available at: https://pubs.acs.org/10.1021/acs.jpca.0c08705

Notes

The authors declare no competing financial interest.

■ ACKNOWLEDGMENTS

This work was supported by the Swedish Research Council and the National Natural Science Foundation of China (21873031). Computer time was generously provided by the Swedish National Infrastructure for Computing. The work was also supported by the Swedish Trygger foundation.

■ REFERENCES

(1) Peters, J. W.; Lanzilotta, W. N.; Lemon, B. J.; Seefedt, L. C. X-ray crystal structure of the Fe-only hydrogenase (Cpl) from Clostridium pasteurianum to 1.8 Ångstrom resolution. *Science* **1998**, *282*, 1853. (Errata: Science 283, 35; 283, 2102.)

(2) Siegbahn, P. E. M.; Tye, J. W.; Hall, M. B. Computational studies of [NiFe] and [FeFe] hydrogenases. *Chem. Rev.* **2007**, *107*, 4414−4435.

(3) Fan, H.-J.; Hall, M. B. A capable bridging ligand for Fe-only hydrogenase: Density functional calculations of a low-energy route for heterolytic cleavage and formation of dihydrogen. *J. Am. Chem. Soc.* **2001**, *123*, 3828−3829.

(4) Liu, Z.-P.; Hu, P. A density functional theory study on the active center of Fe-only hydrogenase: Characterization and electronic structure of the redox states. *J. Am. Chem. Soc.* **2002**, *124*, 5175−5182.

(5) Bruschi, M.; Fantucci, P.; De Gioia, L. DFT investigation of structural, electronic, and catalytic properties of diiron complexes related to the [2Fe](H) subcluster of Fe-only hydrogenases. *Inorg. Chem.* **2002**, *41*, 1421−1429.

(6) Pham, C. C.; Mulder, D. W.; Pelmenschikov, V.; King, P. W.; Ratzloff, M. W.; Wang, H.; Mishra, N.; Alp, E. E.; Zhao, J.; Hu, M. Y.; Tamasaku, K.; Yoda, Y.; Cramer, S. P. Terminal Hydride Species in [FeFe]-Hydrogenases Are Vibrationally Coupled to the Active Site Environment. *Angew. Chem., Int. Ed.* **2018**, *57*, 10605−10609.

(7) Adamska-Venkatesh, A.; Krawietz, D.; Siebel, J.; Weber, K.; Happe, T.; Reijerse, E.; Lubitz, W. New Redox States Observed in [FeFe] Hydrogenases Reveal Redox Coupling Within the H-Cluster. *J. Am. Chem. Soc.* **2014**, *136*, 11339−11346.

(8) Sommer, C.; Adamska-Venkatesh, A.; Pawlak, K.; Birrell, J. A.; Rüdiger, O.; Reijerse, E. J.; Lubitz, W. Proton Coupled Electronic Rearrangement within the H-Cluster as an Essential Step in the Catalytic Cycle of [FeFe] Hydrogenases. *J. Am. Chem. Soc.* **2017**, *139*, 1440−1443.

(9) Reijerse, E. J.; Pham, C. C.; Pelmenschikov, V.; Gilbert-Wilson, R.; Adamska-Venkatesh, A.; Siebel, J. F.; Gee, L. B.; Yoda, Y.; Tamasaku, K.; Lubitz, W.; Rauchfuss, T. B.; Cramer, S. P. Direct Observation of an Iron-Bound Terminal Hydride in [FeFe]-Hydrogenase by Nuclear Resonance Vibrational Spectroscopy. *J. Am. Chem. Soc.* **2017**, *139*, 4306−4309.

(10) Pelmenschikov, V.; Birrell, J. A.; Pham, C. C.; Mishra, N.; Wang, H.; Sommer, C.; Reijerse, E.; Richers, C. P.; Tamasaku, K.; Yoda, Y.; Rauchfuss, T. B.; Lubitz, W.; Cramer, S. P. Reaction Coordinate Leading to H2 Production in [FeFe]-Hydrogenase Identified by Nuclear Resonance Vibrational Spectroscopy and Density Functional Theory. *J. Am. Chem. Soc.* **2017**, *139*, 16894−16902.

(11) Ratzloff, M. W.; Artz, J. H.; Mulder, D. W.; Collins, R. T.; Furtak, T. E.; King, P. W. CO-bridged H-cluster Intermediates in the Catalytic Mechanism of [FeFe] Hydrogenase CaI. *J. Am. Chem. Soc.* **2018**, *140*, 7623.

(12) Birrell, J. A.; Pelmenschikov, V.; Mishra, N.; Wang, H.; Yoda, Y.; Tamasaku, K.; Rauchfuss, T. B.; Cramer, S. P.; Lubitz, W.; DeBeer, S. Spectroscopic and Computational Evidence that [FeFe] Hydrogenases Operate Exclusively with CO-Bridged Intermediates. *J. Am. Chem. Soc.* **2020**, *142*, 222−232.

(13) Haumann, M.; Stripp, S. T. The Molecular Proceedings of Biological Hydrogen Turnover. *Acc. Chem. Res.* **2018**, *51*, 1755−1763.

(14) Mebs, S.; Duan, J.; Wittkamp, F.; Stripp, S. T.; Happe, T.; Apfel, U.-P.; Winkler, M.; Haumann, M. Differential Protonation at the

Catalytic Six-Iron Cofactor of [FeFe]-Hydrogenases Revealed by ^{57}Fe Nuclear Resonance X-ray Scattering and Quantum Mechanics/Molecular Mechanics Analyses. *Inorg. Chem.* **2019**, *58*, 4000−4013.
(15) Mulder, D. W.; Guo, Y.; Ratzloff, M. W.; King, P. W. Identification of a Catalytic Iron-Hydride at the H-cluster of [FeFe]-Hydrogenase. *J. Am. Chem. Soc.* **2017**, *139*, 83−86.
(16) Myers, W. K.; Stich, T. A.; Suess, D. L. M.; Kuchenreuther, J. M.; Swartz, J. R.; Britt, R. D. The Cyanide Ligands of [FeFe] Hydrogenase: Pulse EPR Studies of C-13 and N-15-Labeled H-cluster. *J. Am. Chem. Soc.* **2014**, *136*, 12237.
(17) Liu, T.; Li, B.; Singleton, M. L.; Hall, M. B.; Darensbourg, M. Y. Sulfur Oxygenates of Biomimetics of the Diiron Subsite of the [FeFe]-Hydrogenase Active Site: Properties and Oxygen Damage Repair Possibilities. *J. Am. Chem. Soc.* **2009**, *131*, 8296−8307.
(18) Liu, C.; Liu, T.; Hall, M. B. Influence of the Density Functional and Basis Set on the Relative Stabilities of Oxygenated Isomers of Diiron Models for the Active Site of [FeFe]-Hydrogenase. *J. Chem. Theory Comput.* **2015**, *11*, 205−214.
(19) Stiebritz, M. T.; Reiher, M. Theoretical Study of Dioxygen Induced Inhibition of [FeFe]-Hydrogenase. *Inorg. Chem.* **2009**, *48*, 7127−7140.
(20) Finkelmann, A. R.; Stiebritz, M. T.; Reiher, M. Electric-field effects on the [FeFe]-hydrogenase active site. *Chem. Commun.* **2013**, *49*, 8099−8101.
(21) Greco, C.; Bruschi, M.; Fantucci, P.; Ryde, U.; De Gioia, L. Mechanistic and Physiological Implications of the Interplay among IronSulfur Clusters in [FeFe]-Hydrogenases. A QM/MM Perspective. *J. Am. Chem. Soc.* **2011**, *133*, 18742−18749.
(22) Greco, C.; Bruschi, M.; Fantucci, P.; Ryde, U.; De Gioia, L. Probing the Effects of One-Electron Reduction and Protonation on the Electronic Properties of the Fe-S Clusters in the Active-Ready Form of [FeFe]-Hydrogenases. A QM/MM Investigation. *ChemPhysChem* **2011**, *12*, 3376−3382.
(23) McCullagh, M.; Voth, G. A. Unraveling the Role of the Protein Environment for [FeFe]-Hydrogenase: A New Application of Coarse-Graining. *J. Phys. Chem. B* **2013**, *117*, 4062−4071.
(24) Ginovska-Pangovska, B.; Ho, M.-H.; Linehan, J. C.; Cheng, Y.; Dupuis, M.; Raugei, S.; Shaw, W. J. Molecular dynamics study of the proposed proton transport pathways in [FeFe]-hydrogenase. *Biochim. Biophys. Acta* **2014**, *1837*, 131−138.
(25) Sensi, M.; Baffert, C.; Greco, C.; Caserta, G.; Gauquelin, C.; Saujet, L.; Fontecave, M.; Roy, S.; Artero, V.; Soucaille, P.; Meynial-Salles, I.; Bottin, H.; de Gioia, L.; Fourmond, V.; Léger, C.; Bertini, L. Reactivity of the Excited States of the H-Cluster of FeFe Hydrogenases. *J. Am. Chem. Soc.* **2016**, *138*, 13612−13618.
(26) Siegbahn, P. E. M.; Liao, R.-Z. The energetics of hydrogen molecule oxidation in NiFe hydrogenase. *ACS Catal.* **2020**, *10*, 5603−5613.
(27) Blomberg, M. R. A.; Borowski, T.; Himo, F.; Liao, R.-Z.; Siegbahn, P. E. M. Quantum Chemical Studies of Mechanisms for Metalloenzymes. *Chem. Rev.* **2014**, *114*, 3601−3658.
(28) Becke, A. D. Density-functional thermochemistry. III. The role of exact exchange. *J. Chem. Phys.* **1993**, *98*, 5648−5652.
(29) Siegbahn, P. E. M.; Blomberg, M. R. A. A systematic DFT approach for studying mechanisms of redox active enzymes. *Front. Chem.* **2018**, *6*, 644.
(30) Siegbahn, P. E. M. Water Oxidation Mechanism in Photosystem II, Including Oxidations, Proton Release Pathways, O-O Bond Formation and O_2 Release. *Biochim. Biophys. Acta* **2013**, *1827*, 1003−1019.
(31) *Jaguar*, version 8.9; Schrodinger, Incorporated: New York, NY, 2015. Bochevarov, A. D.; Harder, E.; Hughes, T. F.; Greenwood, J. R.; Braden, D. A.; Philipp, D. M.; Rinaldo, D.; Halls, M. D.; Zhang, J.; Friesner, R. A. Jaguar: A high-performance quantum chemistry software program with strengths in life and materials sciences. *Int. J. Quantum Chem.* **2013**, *113*, 2110−2142.
(32) Grimme, S.; Antony, J.; Ehrlich, S.; Krieg, H. A consistent and accurate ab initio parametrization of density functional dispersion correction (DFT-D) for the 94 elements H-Pu. *J. Chem. Phys.* **2010**, *132*, 154104.
(33) Grimme, S. Semiempirical GGA-type density functional constructed with a long-range dispersion correction. *J. Comput. Chem.* **2006**, *27*, 1787−1799.
(34) Frisch, M. J.; Trucks, G. W.; Schlegel, H. B.; Scuseria, G. E.; Robb, M. A.; Cheeseman, J. R.; Scalmani, G.; Barone, V.; Mennucci, B.; Petersson, G. A.; et al. *Gaussian 09*, Revision C.01, Gaussian, Incorporated: Wallingford CT, 2013.
(35) Pelmenschikov, V.; Blomberg, M. R.; Siegbahn, P. E. A Theoretical Study of the Mechanism for Peptide Hydrolysis by Thermolysin. *J. Biol. Inorg Chem.* **2002**, *7*, 284−298.
(36) Crabtree, R. H.; Siegbahn, P. E. M.; Eisenstein, O.; Rheingold, A. L.; Koetzle, T. F. A New Intermolecular Interaction: Unconventional Hydrogen Bonds with Element-Hydride Bonds as Proton Acceptor. *Acc. Chem. Res.* **1996**, *29*, 348.
(37) Berggren, G.; Adamska, A.; Lambertz, C.; Simmons, T. R.; Esselborn, J.; Atta, M.; Gambarelli, S.; Mouesca, J.-M.; Reijerse, E.; Lubitz, W.; Happe, T.; Artero, V.; Fontecave, M. Biomimetic Assembly and Activation of [FeFe]-Hydrogenase. *Nature* **2013**, *499*, 66−69.
(38) Zhao, Y.; Truhlar, D. G. Design of Density Functionals That Are Broadly Accurate for Thermochemistry, Thermochemical Kinetics, and Nonbonded Interactions. *J. Phys. Chem. A* **2005**, *109*, 5656−5667.
(39) Perdew, J. P.; Ernzerhof, M.; Burke, K. Rationale for mixing exact exchange with density functional approximations. *J. Chem. Phys.* **1996**, *105*, 9982−9985.
(40) Finkelmann, A. R.; Stiebritz, M. T.; Reiher, M. Activation Barriers of Oxygen Transformation at the Active Site of [FeFe] Hydrogenases. *Inorg. Chem.* **2014**, *53*, 11890−11902.

https://dx.doi.org/10.1021/acs.jpca.0c08705
J. Phys. Chem. A 2020, 124, 10540−10549